JOURNAL OF BACTERIOLOGY, May 1987, p. 2055–2062
0021-9193/87/052055-08$02.00/0

Vol. 169, No. 5

Use of On-Section Immunolabeling and Cryosubstitution for Studies of Bacterial DNA Distribution

JAN A. HOBOT,†* MARY-ANN BJORNSTI,‡ AND EDWARD KELLENBERGER

Department of Microbiology, Biozentrum of the University of Basel, CH-4056 Basel, Switzerland

Received 27 October 1986/Accepted 21 February 1987

Escherichia coli **cells were very rapidly frozen and substituted at a low temperature with 3% glutaraldehyde in acetone. Infiltration and embedding with Lowicryl K4M were carried out at −35°C. This procedure resulted in good structural preservation of both the nucleoid morphology and its DNA plasm, such that immunolabeling with the protein-A gold technique could be carried out. With antibodies specific for either double-stranded DNA (dsDNA) or single-stranded DNA (ssDNA), it was shown that dsDNA was present throughout the nucleoid but that ssDNA was located on the nucleoid periphery. Chloramphenicol-treated cells, in which protein synthesis but not DNA replication is stopped, produced a characteristic ringlike nucleoid shape and had both dsDNA and ssDNA present throughout the annular section of the DNA plasm. The relationship between metabolically active DNA and overall bacterial genome organization is discussed.**

In a previous report we showed that bacterial cells prepared for electron microscopy by the cryosubstitution method showed ribosome-free areas filled with grainy and fine fibrillar material (11). By Feulgen analog osmium-ammines staining, we localized DNA within the ribosome-free area. Thus, the bacterial nucleoid was directly analogous with the ribosome-free area. The nucleoid shape seen in cryosubstituted cells was not dependent upon the extracellular salt concentration or upon the chemical fixative contained in the substitution liquid (usually OsO_4 or glutaraldehyde), as had been the case earlier when cultures were fixed directly and prepared by standard techniques (13, 14, 22, 23). The cryosubstitution technique used in the above-mentioned paper (11) involved very rapid freezing of cells to temperatures of liquid helium or propane, substitution with 2.5% OsO_4 in acetone at −90°C, and embedding in Epon, which was then polymerized by heat at 65°C. Extremes of temperature were necessarily involved. However, with the introduction of low-temperature Lowicryl resins (13), these extremes would be avoided in carrying out embedding and polymerization steps (following substitution with a solution of glutaraldehyde in acetone or just acetone) at −35°C (4, 12) or at even lower temperatures, such as −70 or −60°C (4). These resins had two advantages for us: (i) the structural preservation of nucleoid shape and nucleoid content were kept (4), and (ii) immunolabeling studies with the protein A-gold technique (1, 20) could be carried out to localize DNA in further detail. Indeed, a more satisfactory analysis of DNA organization can be performed with antibodies specific for single-stranded DNA (ssDNA) or double-stranded DNA (dsDNA) than with the osmium-ammines method. In this paper we report our results of such an analysis, together with an investigation into changes that occur in DNA distribution during treatment with chloramphenicol, which always causes the nucleoid to assume the shape of a hollow sphere as a consequence of the cessation of protein synthesis.

(Part of these results were presented in a preliminary form earlier [2].)

MATERIALS AND METHODS

Antisera. The antisera used were kind gifts from the following sources. A52 anti-ssDNA (6) and D44 anti-RNA (5) were from D. Eilat (Hadassah University, Jerusalem, Israel). Both are mouse immunoglobulin G (IgG) monoclonal antibodies. A52 IgG antibodies were affinity purified as described by Eilat et al. (6) or were present in cell supernatants containing 20% horse sera. Both sera gave the same results. D44 IgG antibodies were present in cell supernatants containing 20% horse sera. Anti-dsDNA serum from autoimmune mice was donated by R. Franklin (Biozentrum, Basel, Switzerland). Sera from MRL/Mp mice (Olac, Ltd., Bicester, England) were used as a model system for studying lupus erythematosus and produced autoimmune antibodies (IgG) exhibiting high affinities for dsDNA in enzyme-linked immunosorbent assays (18; R. Franklin, personal communication). Sera from BALB/c mice (Olac) which lacked anti-DNA antibodies were also donated by R. Franklin. Affinity-purified mouse IgM monoclonal antibodies specific for ssDNA and dsDNA were from W. Scheer (Deutsches Krebsforschungszentrum, Institut für Experimentelle Pathologie, Heidelberg, Federal Republic of Germany). Affinity-purified goat IgG antibodies to mouse IgM were purchased from Calbiochem-Behring, La Jolla, Calif. (lot no. 401221).

Culture conditions. *Escherichia coli* B was grown in nutrient broth as described previously (10). For chloramphenicol (Parke, Davis & Co., Detroit, Mich.)-treated cells, chloramphenicol (dissolved in 100% ethanol) was added to a 1.5-h culture to produce a final concentration of 25 $\mu g \cdot ml^{-1}$ for 30 to 60 min.

Cryosubstitution. Cells were harvested by filtration, collected on lot no. 807S cigarette paper, and immediately frozen on a liquid helium-cooled copper block (7) as outlined before (10, 11). Substitution of samples was carried out with 3% (vol/vol) glutaraldehyde in pure acetone with a molecular sieve (0.4-nm-pores, Perlform; Merck & Co., Inc., Rahway, N.J.) at −90°C for 86 h. The temperature was then raised to

* Corresponding author.
† Present address: Electron Microscopy Unit, University of Wales College of Medicine, Heath Park, Cardiff CF4 4XN, Great Britain.
‡ Present address: Department of Biochemistry and Molecular Biology, Harvard University, Cambridge, MA 02138.

−35°C, and the samples were kept at −35°C for 6 h. The samples were then embedded in Lowicryl K4M at −35°C by the following protocol: 100% acetone for 1 h, K4M–100% acetone (1:1) for 1 h, K4M–100% acetone (2:1) for 1 h, pure K4M for 1 h, fresh K4M for 1 h, and fresh K4M overnight. On the next day, the samples were either treated with fresh resin for 2 h or put immediately into gelatin capsules and polymerized by indirect UV irradiation (360 nm) for 24 h at −35°C, followed by further hardening at room temperature for 3 days in UV light (13). Thin sections for use in immunolabeling experiments were cut with a diamond knife on an LKB Ultramicrotome III.

Protein A-colloidal gold complex preparation. Colloidal gold (approximate diameter, 14 nm) was prepared by the method of Frens (8) by reduction with sodium citrate. To 80 ml of bidistilled water 0.2 ml of 4% (wt/vol) gold (lot no. 1582; Merck) solution was added, the solution was boiled, 4 ml of 1% (wt/vol) trisodium citrate solution was added, and the solution was mixed gently and allowed to simmer until a red-orange color developed (approximately 8 min). The solution was allowed to cool to room temperature, and the pH was adjusted to 5.8 with 1 M or 0.1 M HCl. With gentle stirring, 1 ml of a 0.5-mg · ml^{-1} solution of protein A (lot no. P8143; Sigma Chemical Co., St. Louis, Mo.) was added to the colloidal gold. After 2 to 3 min, 3.2 ml of 1% (wt/vol) polyethylene glycol (PEG 20000, lot no. 9732; Merck) was added, and the solution was stirred gently for 15 min. The solution was then centrifuged for 1 h at 60,000 × *g* and 4°C, the supernatant was discarded, and the protein A-colloidal gold complex was suspended in 1.5 ml of 0.01 M physiologically buffered saline (PBS, pH 7.4) containing 2 mg of PEG 20000 ml^{-1} and 0.02% (wt/vol) NaN_3 and was stored at 4°C. It is advisable to use siliconized glassware, e.g., 2% (vol/vol) Surfasil (lot no. 42855; Pierce Chemical Co., Rockford, Ill.) in xylol.

Immunolabeling protocols. All immunolabeling experiments were carried out directly on thin-sectioned material resting on copper grids with a 2% collodion film, the grids having been dipped in 0.05% collodion (in amyl acetate) and then quickly dried. This procedure was found to provide very good protection to the copper grids from oxidation during subsequent prolonged exposure to various aqueous solutions. Sera diluted in PBS were used at the following concentrations: A52, 150 μg · ml^{-1}; D44, 1/20 dilution; MRL/Mp and BALB/c, 1/20 dilution; mouse IgM monoclonal antibodies, 110 μg · ml^{-1}; and goat IgG anti-sheep IgM, 50 μg · ml^{-1}. Immunolabeling of sections was carried out at room temperature. Following incubation on a 50-μl drop of 0.5% (wt/vol) ovalbumin in PBS (lot no. 32467; Calbiochem) for 5 min, sections were incubated with the relevant antibody dilution for 1 h. Afer being washed in PBS, the grids were placed on a 50-μl drop of the protein A-colloidal gold complex (1/5 dilution with PBS) for 1 h, washed in PBS and then bidistilled water, and finally stained with 4% (wt/vol) aqueous uranyl acetate for 20 min and Millonig (17) lead acetate for 1 min. With the mouse IgM monoclonal antibodies, following antibody incubation and the PBS wash, an extra step was introduced, namely, incubation with goat IgG anti-mouse IgM for 1 h. Controls were carried out in the following way: (i) protein A-colloidal gold alone, with the 1-h antibody incubation being replaced by a 1-h PBS treatment; (ii) as for (i) but including incubation with goat IgM to anti-mouse IgM for 1 h; (iii) preincubation of A52 with DNA, of D44 with RNA, and of mouse IgM with DNA or RNA for 30 min (solutions of DNA [1 μg · ml^{-1}] from *E. coli* B [lot no. D2001; Sigma] and RNA [1 μg · ml^{-1}] from *E. coli* 16S and 23S rRNAs [lot no. 206938; Boehringer Mannheim Biochemicals, Indianapolis, Ind.] were made up in PBS; after the preincubation step, the immunolabeling protocol was followed); and (iv) preincubation of MRL/Mp serum with calf thymus DNA-cellulose prior to immunolabeling. All sections were examined in a Zeiss EM109 electron microscope operating at 80 kV.

RESULTS

Results of the various DNA localization experiments are shown in Fig. 1 to 6.

DNA localization in untreated cells. DNA can be either ssDNA or dsDNA. We therefore used in our study antibodies directed against both types. The results of on-section immunolabeling with A52 mouse monoclonal antibodies specific for ssDNA are shown in Fig. 1. A ribosome-free area having a cleft, lobular shape was present within the cytoplasm. It contained grains intermingled with fibrous elements (Fig. 3 and 4). The gold label in both Fig. 1a and 1b was along the periphery of the ribosome-free area, perhaps tending to be in the more cleft regions of this area. When serum from MRL/Mp mice was used, the antibodies being specific for dsDNA, a different result was obtained (Fig. 2). The gold label not only was on the periphery of the ribosome-free area but also was distributed throughout the area. Further, the clear appearance of the ribosome-free area in the cytoplasm in Fig. 1 was now superseded by a strong "serum staining" in Fig. 2 covering the ribosome-free area and giving it a greyish appearance. This phenomenon was more striking in chloramphenicol-treated cells (Fig. 5b). Indeed, we found that for this particular MRL/Mp serum, no gold label was required to demonstrate dsDNA localization. Preincubation of the MRL/Mp serum with calf thymus DNA-cellulose prior to immunolabeling produced no specific gold labeling of the ribosome-free area and produced only the normal uranyl acetate staining of this area (Fig. 6b), as was also demonstrated by comparing Fig. 1, 3, and 4 with the serum-stained cells of Fig. 2. Immunolabeling with serum from BALB/c mice, which do not produce anti-DNA autoimmune antibodies, produced the same result as that seen in Fig. 6b. Controls for the staining of ssDNA with A52 consisted of serum preincubated with DNA prior to labeling. They showed no specific labeling of ssDNA (Fig. 6a). However, preincubation with RNA still produced specific labeling on the ribosome-free area periphery (results not shown). The very interesting serum staining phenomenon, described here for the first time, seems to involve a protein component of the serum which has a high affinity for DNA. Further experiments are being carried out to determine what causes this staining and whether it is specific only for the MRL/Mp serum.

DNA localization was demonstrated with a third type of antibody, mouse IgM monoclonal antibodies specific for both ssDNA and dsDNA. Figure 3 shows that no serum staining of the bacteria occurred and that the gold label was located in the ribosome-free area, with more label distributed in the peripheral regions of the area. Preincubation of the serum with DNA removed the label (Fig. 6c). (As Fig. 6c is of a chloramphenicol-treated cell, it can also be compared with Fig. 5c.)

To show that the ribosome-free area was not the only area that was labeled, we applied D44 serum specific for RNA to bacterial thin sections (Fig. 4). The gold label was located over the ribosomes and along the periphery of the ribosome-free area but was not located over the ribosome-free area.

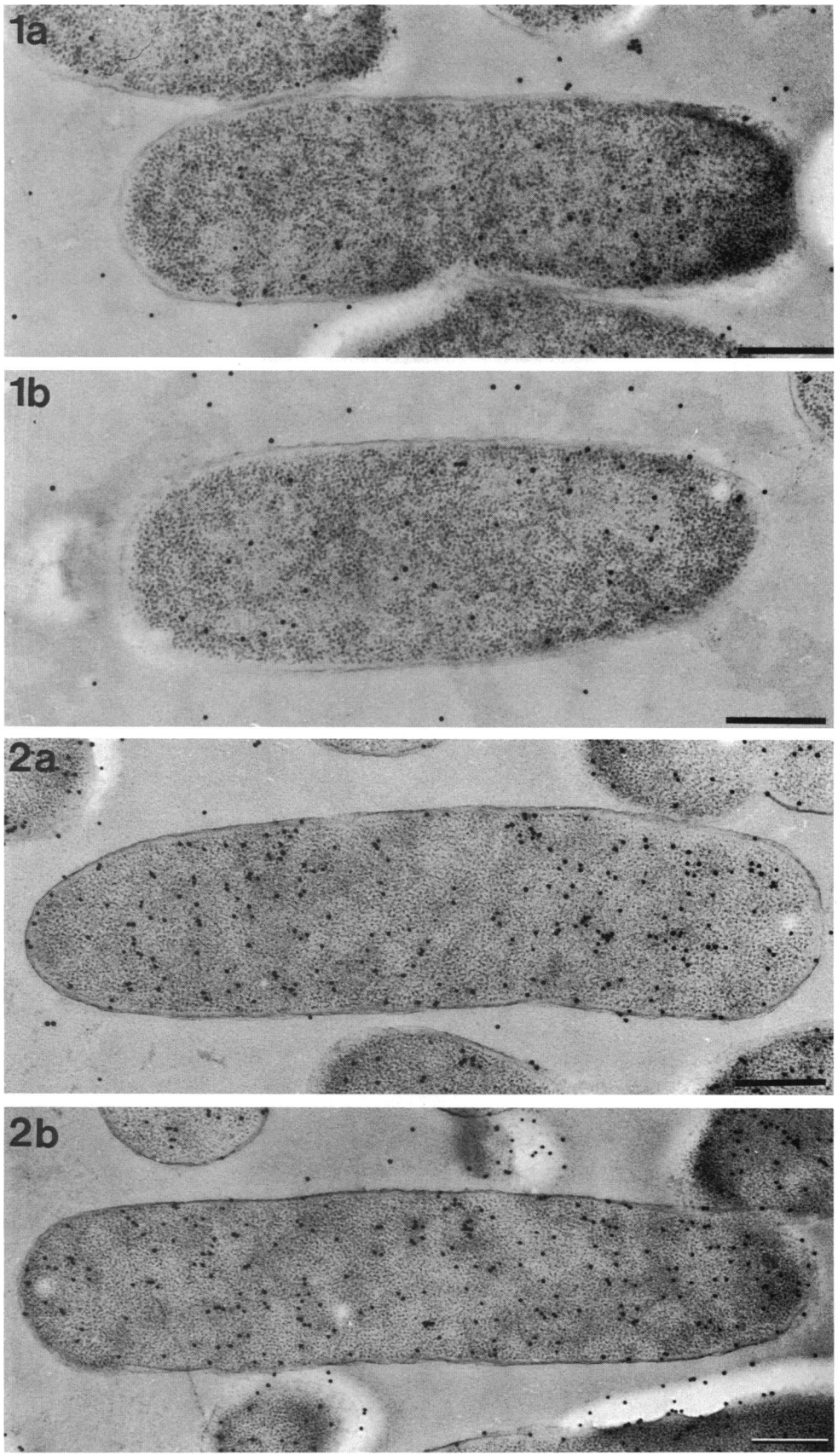

FIG. 1. *E. coli* B labeled with A52 anti-ssDNA monoclonal antibodies. The gold label is situated on the periphery of the ribosome-free area, which has a cleft, lobular appearance and grainy and fine fibrillar contents. Bars, 0.5 μm.

FIG. 2. *E. coli* B labeled with MRL/MP anti-dsDNA serum. The gold label is located over the ribosome-free area, which appears greyish because of the phenomenon of serum staining. Bars, 0.5 μm.

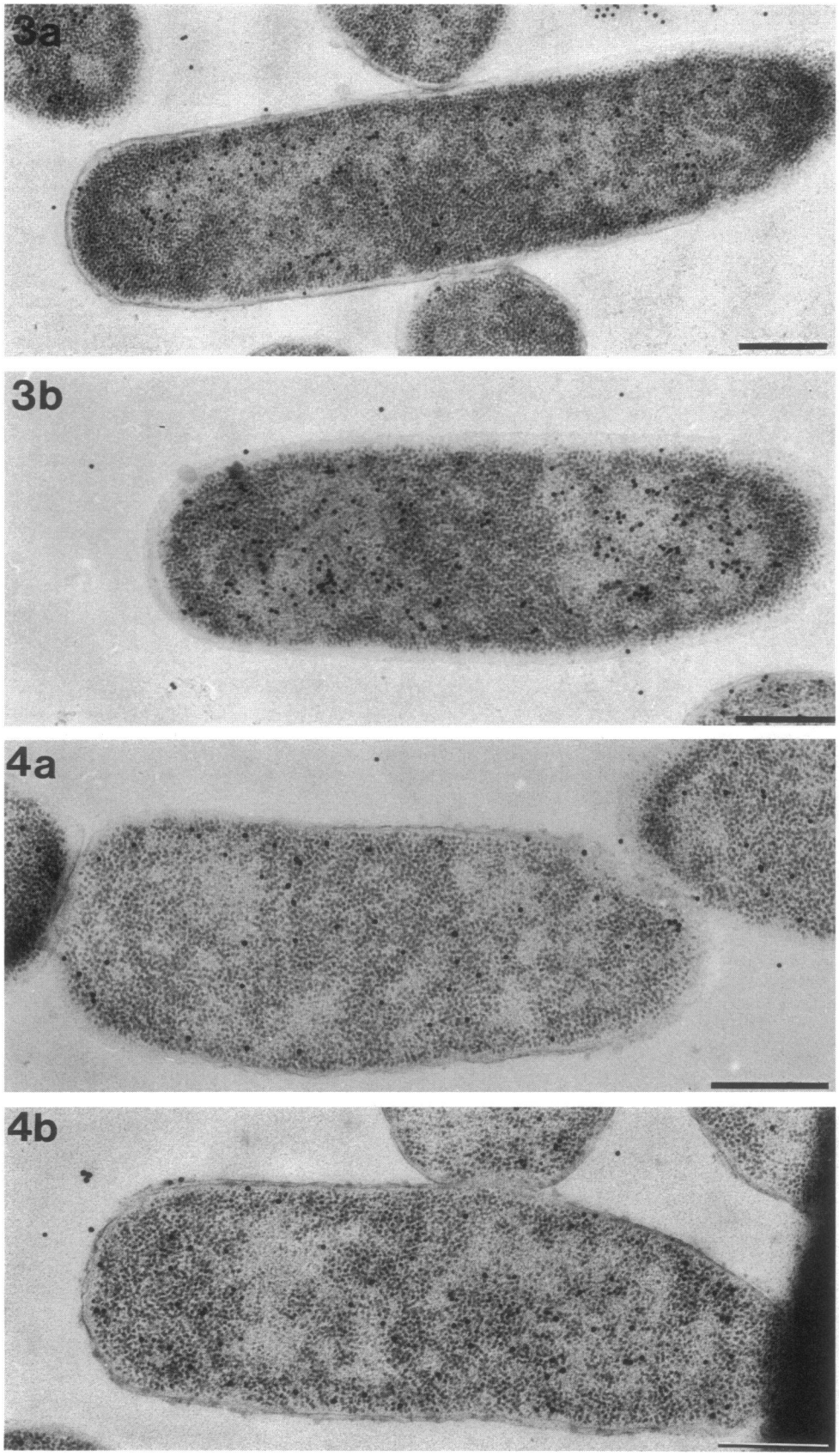

FIG. 3. *E. coli* B labeled with mouse IgM monoclonal antibodies directed against ssDNA and dsDNA. The gold particles are distributed over the ribosome-free area but tend to be more localized on the periphery of this area. Bars, 0.5 μm.

FIG. 4. *E. coli* B labeled with D44 anti-RNA serum. The gold label is found only in the cytoplasm or ribosomal area. Bars, 0.5 μm.

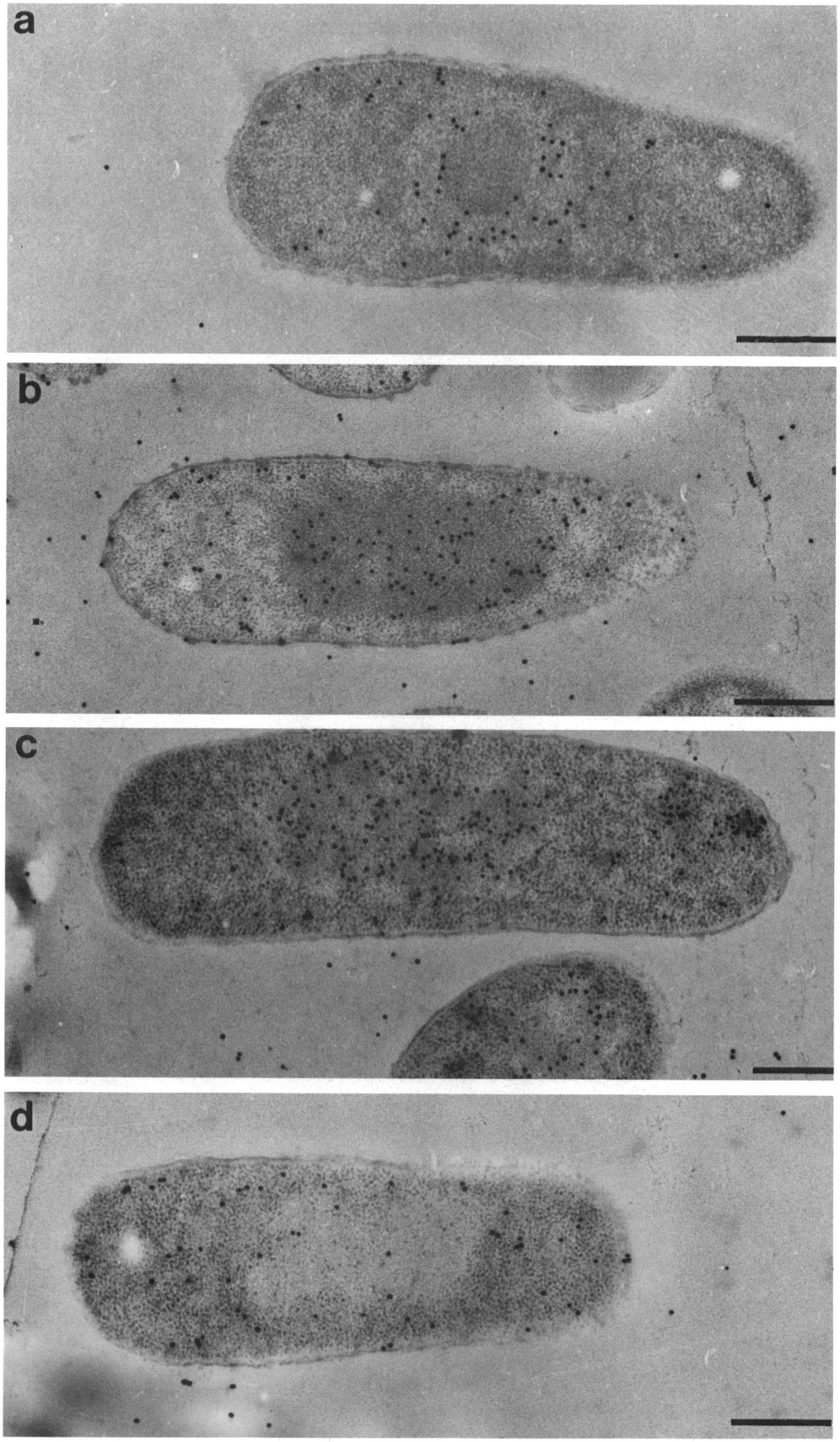

FIG. 5. *E. coli* B treated with chloramphenicol (25 μg · ml^{-1}) for 1 h. (a) Labeling with A52 anti-ssDNA. The typical hollow, spherical or doughnut ribosome-free area nucleoid is seen. The gold particles are present throughout the ribosome-free area. Bar, 0.5 μm. (b) Labeling with MRL/Mp anti-dsDNA serum. Again, the gold label is located over the whole ribosome-free area. Also, the serum staining phenomenon of the ribosome-free area is strikingly seen. Bar, 0.5 μm. (c) Labeling with mouse IgM monoclonal antibodies against ssDNA and dsDNA. The gold label is located over the whole ribosome-free area. However, as in panels a and b, there is some label in the cytoplasm. Bar, 0.5 μm. (d) Labeling with D44 anti-RNA serum. The gold label is confined to the cytoplasm. Bar, 0.5 μm.

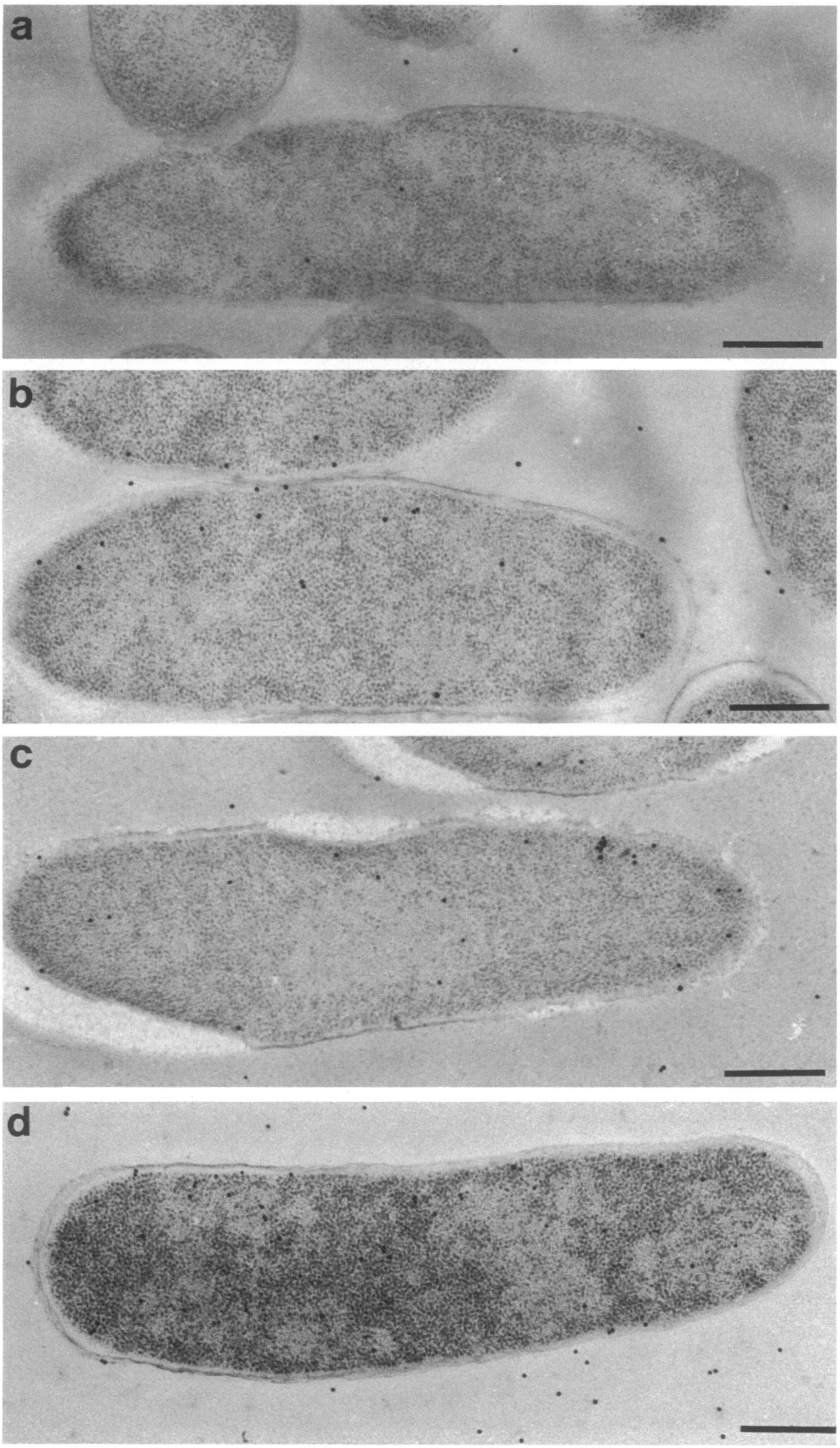

FIG. 6. Control experiment for immunolabeling. See the text for full details. (a) A52 anti-ssDNA preincubated with DNA. No specific labeling occurred. Bar, 0.5 μm. (b) MRL/Mp anti-dsDNA serum preincubated with calf thymus DNA-cellulose. No specific labeling occurred, and normal uranyl acetate staining returned. Bar, 0.5 μm. (c) Mouse IgM monoclonal antibodies against ssDNA and dsDNA preincubated with DNA. No specific labeling occurred. Bar, 0.5 μm. (d) D44 anti-RNA serum preincubated with RNA. There was some labeling in the cytoplasm; compare with Fig. 4. Bar, 0.5 μm.

TABLE 1. Intracellular distribution of colloidal gold particles in cells immunolabeled with MRL/Mp sera

No. of micrographs	Avg no. of gold particles/μm^2 in[a]:		
	Ribosome-free area	Cytoplasm	Background
13	59.6 ± 10.2	4.7 ± 1.3	2.5 ± 0.9
3	128.3 ± 17.9	13.1 ± 5.3	10.6 ± 0.8

[a] Data were determined with a Numonics Corp. electronic graphics calculator coupled to an Apple computer.

Preincubation with rRNA removed most of the label (Fig. 6d) but not all of it, with more of the remaining label being along the periphery of the ribosome-free area, raising the question of antibody specificities directed against rRNA and mRNA in the cytoplasm. Earlier tests of D44 antibodies were directed against rRNA (5, 6). A control experiment involving preincubation with DNA resulted in labeling solely over the ribosomes (results not shown).

DNA localization in chloramphenicol-treated cells. The specific ringlike, annular or doughnut shape of the ribosome-free area following chloramphenicol treatment is shown in Fig. 5a. When immunolabeling was done with A52 anti-ssDNA antibodies, the gold label was not on the periphery of the ribosome-free areas, as it was in untreated cells (Fig. 1), but was present throughout the ribosome-free area (Fig. 5a). This was also the case for MRL/Mp anti-dsDNA serum (Fig. 5b) and mouse IgM monoclonal antibodies directed against ssDNA and dsDNA (Fig. 5c). There was some label in the cytoplasm, perhaps associated with remnants of the ribosome-free area. Labeling chloramphenicol-treated cells with D44 anti-RNA resulted in the label being restricted mainly to the cytoplasm (Fig. 5d). We have found no labeling as yet in the central circle of the doughnut, which ultrastructurally sometimes resembles ribosomes but does not respond to anti-RNA-specific antibodies.

Quantitation. Looking at gold particle distributions necessitates finding out how many gold particles are in the ribosome-free area and how many are in the cytoplasm. For gold particle distributions along the periphery of the ribosome-free area, one must also find out how far into the cytoplasm or how far into the area a particle has to be to be dismissed as being located peripherally. This determination will depend upon particle size, antibody and antigen sizes, and how the antibody-antigen complex and the gold particle are positioned on the section surface. We have avoided making these determinations in this study by looking instead at the reproducibility of peripheral locations, the results presented here being samples from five experiments, and also by establishing appropriate control experiments, including protein A-gold complex alone, which in all cases produced no specific labeling. However, when the label was located over the ribosome-free area, as in MRL/Mp-treated sections, gold particle counts were carried out (Tables 1 and 2). Most of the anti-dsDNA was restricted to the ribosome-free area (Table 1). Cytoplasmic labeling was just over the background level and was thus negligible. However, with chloramphenicol-treated cells (Table 2), the label was mainly in the ribosome-free area, but there was just a small amount in the cytoplasm, significantly over the background level.

DISCUSSION

The results presented in this paper illustrate the good level of structural preservation that can be achieved by the cryosubstitution method and (coupled with the results of immunolabeling investigations) demonstrate how clearly the location of a specific label can be matched to ultrastructural details. By eliminating the need for prior chemical fixation of a bacterial culture, cryosubstitution as a procedure for preparing specimens for immunolabeling has two advantages. (i) Structures sensitive to chemical fixatives, which cause their rearrangement (e.g., the bacterial nucleoid), or sensitive to subsequent dehydration irrespective of whether room or low temperatures are used (e.g., bacterial DNA plasm) can be fixed physically by freezing (11). (ii) Antigenic sites sensitive to chemical fixatives and so rendered useless for immunolabeling analysis may be frozen rapidly and substituted with just acetone alone at −90°C, followed by resin infiltration and polymerization at very low temperatures (−70 to −60°C) with the new Lowicryl HM23 or K11M (4). The latter is an extrapolation from results obtained with K4M: bacteria were frozen, substituted with just acetone, and embedded at −35°C; they showed a well-preserved ultrastructure (J. A. Hobot, unpublished results). However, this approach, using both freezing and low-temperature technologies, should only be applied for specimens which cannot be prepared for immunolabeling either (i) by the progressive-lowering-of-temperature technique with Lowicryl resins (3), designed also for use at either 4°C or room temperatures with either UV light or chemical polymerization (3, 13), or (ii) with other suitable resins (e.g., LR White [19]).

The immunolabeling data presented in this report show that the bacterial nucleoid (ribosome-free area of the cell) contains dsDNA and that ssDNA is located at the periphery of the nucleoid. It is the ssDNA which is transcribed, therefore probably accounting for its proximity to the ribosomes. This is consistent with the results of Miller and Hamalko (16), who demonstrated that metabolically active DNA, when observed isolated under the electron microscope, had mRNA branches studded with ribosomes coming off of it. The close proximity of metabolically active DNA to ribosomes was also suggested earlier by Kleppe et al. (15) and in a schematic diagram by J. Gumpert (see Fig. 10 in Hobot et al. [11]). Bjornsti et al. (2), using the methods outlined in this paper, found that a bacterial DNA-binding protein, HU, was also located on the periphery of the nucleoid. Further studies involving RNA polymerase to-

TABLE 2. Intracellular distribution of colloidal gold particles in chloramphenicol (25 $\mu g \cdot ml^{-1}$)-treated cells immunolabeled with MRL/Mp sera

Length of chloramphenicol treatment (min)	No. of micrographs	Avg no. of gold particles/μm^2 in[a]:		
		Ribosome-free area	Cytoplasm	Background
30	5	103.0 ± 13.3	16.2 ± 2.8	6.1 ± 5.4
60	5	115.6 ± 8.1	13.7 ± 2.9	3.2 ± 0.4

[a] See Table 1, footnote *a*.

gether with DNA gyrase and topoisomerase, enzymes responsible, respectively, for introducing (9) or removing (21) supercoils in DNA, revealed a similar peripheral location and will be reported elsewhere (manuscript in preparation). Taken together, these various pieces of information suggest that perhaps ssDNA forms transcription-translation complexes with one or more enzymes on the nucleoid periphery.

The determination of whether such complexes exist needs more investigation with, perhaps, immunolabeling studies carried out on relevant mutants lacking one or more of the above-mentioned enzymes or studies of the effects on cells of antibiotics which induce specific metabolic changes in cells or changes in nucleoid morphology or both. As an example, we presented some labeling data for chloramphenicol-treated cells, in which protein synthesis is arrested but in which DNA replication continues until its cycle is completed. Also, the nucleoid changes shape into an annular form. (At the dose used in this study, 25 $\mu g \cdot ml^{-1}$, once the chloramphenicol is removed, the cells recover and grow, and the normal nucleoid morphology is observed again.) In these chloramphenicol-treated cells, the ssDNA is now no longer on the nucleoid periphery but is present with dsDNA throughout the annular structure of the nucleoid (cf. Fig. 5a and b). If there is a high turnover of one or more of the proteins suggested to be involved in the transcription-translation complex, then the complex could be weakened so as to become released from a ribosomal association, with the nucleoid assuming the shape of a hollow sphere. Identifying which proteins are important in stabilizing or activating the complex or both and simultaneous localizing these proteins are likely to lead to new insights into the organization and functioning of the bacterial genome.

ACKNOWLEDGMENTS

Particular thanks are due to Werner Villiger, who set up and partly designed the instruments for cryosubstitution. He also helped us with the experiments. We thank Marianne Schäfer for typing the successive versions of the manuscript and Chantal Laburte-Becker for the protein A-gold preparation recipe.

LITERATURE CITED

1. **Bendayan, M.** 1984. Protein A-gold microscopic immunocytochemistry: methods, applications, and limitations. J. Electron Microsc. Techniques **1**:243–270.
2. **Bjornsti, M. A., J. A. Hobot, A. S. Kelus, W. Villiger, and E. Kellenberger.** 1986. New electron microscopy data on the structure of the nucleoid and their funcational consequences. *In* C. Gualerzi (ed.), Bacterial chromatin. Springer Verlag KG, Berlin.
3. **Carlemalm, E., R. M. Garavito, and W. Villiger.** 1982. Resin development for electron microscopy and an analysis of embedding at low temperature. J. Microsc. (Oxford) **126**:123–143.
4. **Carlemalm, E., W. Villiger, J. A. Hobot, J.-D. Acetarin, and E. Kellenberger.** 1985. Low temperature embedding with Lowicryl resins: two new formulations and some applications. J. Microsc. (Oxford) **140**:55–63.
5. **Eilat, D., M. Hochberg, R. Fischel, and R. Laskov.** 1982. Antibodies to RNA from autoimmune NZB/NZW mice recognize a similar antigenic determinant and show a large iodiotypic diversity. Proc. Natl. Acad. Sci. USA **79**:3818–3822.
6. **Eilat, D., M. Hochberg, J. Pumphrey, and S. Rudikoff.** 1984. Monoclonal antibodies to DNA and RNA from NZB/NZW F_1 mice: antigenic specificities and NH_2 terminal amino acid sequences. J. Immunol. **133**:489–494.
7. **Escaig, J.** 1982. New instruments which facilitate rapid freezing at 83K and 6K. J. Microsc. (Oxford) **126**:221–229.
8. **Frens, G.** 1973. Controlled nucleation for the regulation of the particle size in monodisperse gold solutions. Nature (London) Phys. Sci. **241**:20–22.
9. **Gellert, M., K. Mizuuchi, M. H. O'Dea, and H. Nash.** 1976. DNA gyrase: an enzyme that introduces superhelical turns into DNA. Proc. Natl. Acad. Sci. USA **73**:3872–3876.
10. **Hobot, J. A., E. Carlemalm, W. Villiger, and E. Kellenberger.** 1984. Periplasmic gel: new concept resulting from the reinvestigation of bacterial cell envelope ultrastructure by new methods. J. Bacteriol. **127**:143–152.
11. **Hobot, J. A., W. Villiger, J. Escaig, M. Maeder, A. Ryter, and E. Kellenberger.** 1985. Shape and fine structure of nucleoids observed on sections of ultrarapidly frozen and cryosubstituted bacteria. J. Bacteriol. **162**:960–971.
12. **Humbel, B., T. H. Marti, and M. Müller.** 1983. Improved structural preservation by combining freeze substitution and low temperature embedding, p. 585–594. *In* G. Pfefferkorn (ed.), BEDO, vol. 16. EDO, Antwerp, Belgium.
13. **Kellenberger, E., E. Carlemalm, W. Villiger, J. Roth, and R. M. Garavito.** 1980. Low denaturation embedding for electron microscopy of thin sections. Chemische Werke Lowi GmbH, Waldkraiburg, Federal Republic of Germany.
14. **Kellenberger, E., and A. Ryter.** 1964. In bacteriology, p. 335–393. *In* B. M. Siegel (ed.), Modern developments in electron microscopy. Academic Press, Inc. (London), Ltd., London.
15. **Kleppe, K., S. Overbo, and I. Lossius** 1979. The bacterial nucleoid. J. Gen. Microbiol. **112**:1–13.
16. **Miller, O. L., and B. A. Hamalko.** 1972. Visualisation of RNA synthesis of chromosomes. Int. Rev. Cytol. **33**:1–25.
17. **Millonig, G.** 1961. A modified procedure for lead staining of thin sections. J. Biophys. Biochem. Cytol. **11**:736–739.
18. **Munns, T. W., M. K. Liszewski, and B. H. Hahn.** 1984. Antibody-nucleic acid complexes. Antigenic domains within nucleosides as defined by solid-phase immunoassay. Biochemistry **23**:2958–2964.
19. **Newman, G. R., B. Jasani, and E. D. Williams.** 1983. A simple post-embedding system for the rapid demonstration of tissue antigens under the electron microscope. Histochem. J. **15**: 543–555.
20. **Roth, J. R., M. Bendayan, E. Carlemalm, W. Villiger, and R. M. Garavito.** 1982. The enhancement of structural preservation and immunocytochemical staining in low temperature embedded pancreatic tissue. J. Histochem. Cytochem. **29**:663–671.
21. **Wang, J. C.** 1971. Interaction between DNA and an *Escherichia coli* protein. J. Mol. Biol. **55**:523–533.
22. **Whitfield, J. F., and R. G. E. Murray.** 1956. The effects of the ionic environment on the chromatin structures of bacteria. Can. J. Microbiol. **2**:245–260.
23. **Woldringh, C. L.** 1973. Effect of cations on the organisation of the nucleoplasm in *Escherichia coli* prefixed with osmium tetroxide or glutaraldehyde. Cytobiologie **8**:97–111.